Available online at www.sciencedirect.com
ScienceDirect
Journal of Power Sources 161 (2006) 492–502
JOURNAL OF POWER SOURCES
www.elsevier.com/locate/jpowsour

Steady state and dynamic performance of proton exchange membrane fuel cells (PEMFCs) under various operating conditions and load changes

Qiangu Yan [a,*], H. Toghiani [b], Heath Causey [a]

[a] *Center for Advanced Vehicular Systems (CAVS), Box 5405, Mississippi State University, MS 39762-5405, United States*
[b] *Dave C. Swalm School of Chemical Engineering, Box 9595, Mississippi State University, MS 39762, United States*

Received 21 January 2006; received in revised form 13 March 2006; accepted 28 March 2006
Available online 5 May 2006

Abstract

The steady-state performance and transient response for H_2/air polymer electrolyte membrane (PEM) fuel cells are investigated in both single fuel cell and stack configurations under a variety of loading cycles and operating conditions. Detailed experimental parameters are controlled and measured under widely varying operating conditions. In addition to polarization curves, feed gas flow rates, temperatures, pressure drop, and relative humidity are measured. Performance of fuel cells was studied using steady-state polarization curves, transient *I–V* response and electrochemical impedance spectroscopy (EIS) techniques. Different feed gas humidity, operating temperature, feed gas stoichiometry, air pressure, fuel cell size and gas flow patterns were found to affect both the steady state and dynamic response of the fuel cells. It was found that the humidity of cathode inlet gas had a significant effect on fuel cell performance. The experimental results showed that a decrease in the cathode humidity has a detrimental effect on fuel cell steady state and dynamic performance. Temperature was also found to have a significant effect on the fuel cell performance through its effect on membrane conductivity and water transport in the gas diffusion layer (GDL) and catalyst layer. The polarization curves of the fuel cell at different operating temperatures showed that fuel cell performance was improved with increasing temperature from 65 to 75 °C. The air stoichiometric flow rate also influenced the performance of the fuel cell directly by supplying oxygen and indirectly by influencing the humidity of the membrane and water flooding in cathode side. The fuel cell steady state and dynamic performance also improved as the operating pressure was increased from 1 to 4 atm. Based on the experimental results, both the steady state and dynamic response of the fuel cells (stack) were analyzed. These experimental data will provide a baseline for validation of fuel cell models.

Keywords: PEMFCs; Performance; Transient response; Various conditions

1. Introduction

Fuel cells have attracted great attention in recent years as a promising replacement for traditional internal combustion engines due to their high power density and ultra-low emissions [1–3]. Though significant improvements in polymer electrolyte membrane (PEM) fuel cell technology has been achieved over the past decade, the performance, stability, reliability, and cost for today's fuel cell technology is not sufficient to replace the internal combustion engine [4–6]. A number of fundamental problems must be overcome to improve their performance and reduce their cost. The objectives for further development of fuel cells include: to identify critical issues, such as what are the effects of start-up, shut-down, and transient response; to identify key parameters for fuel cell performance and examine how to optimize stack and system design; and examine performance under extreme conditions, such as sub-freezing temperatures. It is important to study the dynamic behavior of fuel cells to obtain stable performance under various operating conditions. In particular, knowledge of the dynamic behavior is critical to the engineering and design of the fuel cells, stacks, and systems [7]. A control system is needed to ensure that the flow rate and temperature of fuel and air are within prescribed limits during normal operation at variable loads, as well as during system start-up and shut-down. Dynamic behavior is the most important aspect of fuel cell operation that should be studied under wide operating conditions. The control, design, and optimum operation of fuel cells require an understanding of their dynamics when there are changes in current, voltage, or power [8]. Fuel cell dynamic response is very important; unfortunately,

* Corresponding author. Tel.: +1 662 325 5906; fax: +1 662 325 5433.
E-mail address: yan@cavs.msstate.edu (Q. Yan).

0378-7753/$ – see front matter © 2006 Elsevier B.V. All rights reserved.
doi:10.1016/j.jpowsour.2006.03.077

there are few publications describing the dynamic behavior of PEM fuel cells under various operating conditions. Some work has been preformed on the dynamic response of PEM and direct methanol fuel cells (DMFC) through experimental methods [9–16]. Hamelin et al. [9] investigated the behavior and performance of a proton exchange membrane (PEM) fuel cell under fast load commutations. It was found that the fuel cell system response was faster than 0.15 s to load commutations; however, load transients were present in the voltage and current response. Morner et al. [10] experimentally evaluated the dynamic behavior of an air-breathing fuel cell. The performance of an air-breathing PEM fuel cell has been experimentally measured to investigate the steady state and transient effects of temperature, humidity, and air flow rate. Kim et al. [11,12] examined the effect of stoichiometry, reservoirs, and fuel dilution on the dynamic behavior of a PEM fuel cell during load change. Overshoot and undershoot behavior of the steady state current density was observed for various rates of change in the voltage at a constant inlet flow rate. Argyropoulos et al. [13,14] investigated the influential parameters for a liquid-fed DMFC and showed experimentally the impact of anode concentration, flow, and cathode pressure on the dynamic fuel cell response.

Many mathematical models of PEM fuel cells can be found in the literature [15–23]. The earliest and most cited models were developed by Springer et al. [15], and Bernardi and Vebrugge [16,17]. The first one-dimensional fuel cell model was by Springer et al. [15] at Los Alamos National Laboratory (LANL). This model was an isothermal, one-dimensional, steady state model that considered polarization and electrode effects through the polarization equation. In the model, water diffusion coefficients, electro-osmotic drag coefficient, water sorption isotherms, and membrane conductivity were measured as a function of the membrane water content. The model predicted an increase in membrane resistance with increased current density and demonstrated the great advantage of a thinner membrane in alleviating the resistance problem. The Bernardi and Verbrugge model [16,17] assumed a fully hydrated membrane and incorporated porous-electrode equations and Stefan–Maxwell diffusion in the diffusion media and catalyst layers. The model of Springer et al. [15] did not use porous-electrode equations but did consider changing water content in the membrane. The other important early fuel cell models included those by Fuller and Newman [18] and Nguyen and White [19]. These models examined flow effects along the channel. Their models treated the membrane as a two-phase system similar to a porous medium, where there were separate gas and liquid channels, and the porosity remained constant. Liu and co-workers [20] performed the first two-dimensional computational fluid dynamics (CFD) analysis of a PEM fuel cell. Wang and Savinell [21] first applied a CFD model to liquid water transport in the porous gas diffusion layer. The liquid water and gaseous species governing equations were primarily coupled by an interfacial mass-transfer rate. Nguyen and co-workers also performed notable work in developing fuel cell models [22,23].

The earliest dynamic fuel cell models were developed by Amphlett et al. [24,25] for predicting transient responses of PEM fuel cells. The transient models can predict fuel cell performance in terms of fuel cell voltage output and heat losses as a function of time due to various changes imposed on the fuel cell system. Um et al. [26] developed a transient, multidimensional model to simulate PEM fuel cells. The model accounts simultaneously for electrochemical kinetics, current distribution, hydrodynamics, and multi-component transport. Ceraolo et al. [27] developed a simplified dynamic model of a PEM fuel cell based on physicochemical knowledge of the phenomena occurring inside the fuel cell. The model has been implemented in the MATLAB/SIMULINK environment. Sundmacher et al. [28] used a mathematical approach for the liquid DM fuel cell under dynamic load conditions. Kulikovsky [29] described analytically the gas dynamics in channels of a gas-fed DM fuel cell and Xu et al. [30] examined a DM fuel cell model that captures the essence of electrode kinetics and methanol crossover through the membrane. Berning and Djilali [31] presented a computational fluid dynamics multiphase model of a PEM fuel cell. The model accounted for three-dimensional (3D) transport processes with phase change and heat transfer in the gas-diffusion layers, the gas flow channels, and the cooling channels. Xue et al. [32] developed a system-level dynamic model of a PEM fuel cell capable of characterizing the effects of temperature, gas flow, and capacitance with particular emphasis focused on system transient behavior. Shimpalee et al. [33,34] presented a three-dimensional numerical simulation of the transient response of a PEM fuel cell (PEMFC) subjected to a variable load. The predictions showed transients in the current density that overshoot the final state value when the fuel cell voltage was abruptly changed from 0.7 to 0.5 V for fixed excess initial stoichiometric flow rates. Yu et al. [35] developed a water and thermal management model for a Ballard PEM fuel cell. The model provided information regarding the reaction products (i.e., water and heat), stack power, stack temperature, and system efficiency, thereby assisting the designer in achieving the best thermal and water management. Wang and Wang [36,37] developed a three-dimensional, transient model to study the transient dynamics of PEM fuel cell operation. The results showed that the time for fuel cells to reach steady state was on the order of 10 s due to the effect of water accumulation in the membrane, consistent with theoretical estimations.

Though significant progress has been made in PEM fuel cell, modeling during the past ten years, some key problems still exist. Key issues in modeling PEM fuel cell systems include: (i) balancing the complexity of the model (computing time) with realism, and applicability of model; (ii) detailed verification of the model is often difficult; (iii) lack of measurement techniques, especially real time (in situ) and non-intrusive techniques; (iv) lack of existing fuel cell systems and performance data. Along with these issues, how to validate the model is perhaps the most difficult and challenging issue. A series of bulk validations have been done for validating the fuel cell models by comparison of simulation results to the fuel cell polarization curves [38–40]. These authors validated their models by comparing experimentally measured fuel cell polarization curves with their predicted fuel cell current. Some researchers have

tried to validate their fuel cell models by comparing the current density distribution, temperature distribution, and reactant species distribution predicted by fuel cell models to experimental data [41–44]. However, detailed validation is still developing because of a general lack of real time and non-intrusive measurement techniques. More work is required in the areas of modeling, measurement methods and fuel cell design optimization based on a judicious selection of available approaches [45]. In the present work, detailed experimental parameters are controlled and measured under widely varying operating conditions. In addition to the polarization curves, feed gas flow rates, temperatures, pressure, relative humidity are all measured. The effects of relative humidity, temperature, feed gas stoichiometry and air pressure on both fuel cell steady state and dynamic behavior are investigated. The dynamic behavior of a small fuel cell stack dynamic behavior is also examined. The experimental data provide a baseline for validation of fuel cell models.

2. Experimental

2.1. Experimental set up

The following experiments were performed using a fuel cell test bed system that was designed and constructed at the Center for Advanced Vehicular Systems located on the campus of Mississippi State University. This test bed was used to investigate fuel cell steady state and transient behaviors of several different single membrane fuel cells and a multiple membrane fuel cell stack. The single membrane fuel cells used in this experiment include a 5 cm^2 fuel cell with a single serpentine flow pattern, 5 cm^2 fuel cell with a triple serpentine flow pattern, 5 cm^2 fuel cell with a parallel flow pattern, and 25 cm^2 fuel cell with a triple serpentine flow pattern. The fuel cell stack tested in the experiments contained eight individual membranes with each membrane having an active area of 49 cm^2. Fuel cell performance was evaluated at operating temperatures from subzero to 85 °C, pressures from 1 to 4 atm, and humidity levels from 0% to 100% for both reactant gases. Pure hydrogen and air were used as reactant gases which were humidified by passing each through an external humidifier. Temperatures of gas lines between the humidifiers and the fuel cell and between the fuel cell and dew point meters were maintained at 95 °C.

2.2. Preparation of MEA and assembly of single fuel cells

The catalyst ink for the electrodes were prepared by mixing the catalyst powders (20 wt.% Pt/C, E-Tek), 5% Nafion solution, and isopropyl alcohol. Then the prepared catalyst ink was sprayed on to the water proof carbon paper and carbon cloth to achieve a platinum loading of 0.4 mg cm^{-2} for both the anode and cathode. Each membrane electrode assembly (MEA) was fabricated by placing the electrodes on both sides of the pretreated Nafion 112, 115 and 117 membranes and then hot pressing the MEA at 140 °C and 200 kg cm^{-2} for 4 min.

2.3. Steady state and dynamic behaviors of the fuel cell under various conditions

The load across the fuel cell was controlled and measured with a TDI-Dynaload RBL488 series electronic load. The electronic load's minimum response time of 10 μs was sufficient for all steady state and dynamic tests performed on the fuel cells. Each variation of operating conditions was investigated by performing measurements of polarization behavior, transient response, and AC impedance of the fuel cell. Polarization curves were obtained by stepping the current density, allowing the fuel cell to stabilize, and measuring the fuel cell voltage. The transient response measurement was performed by abruptly changing the current density and measuring the time response of the voltage across the fuel cell. The ac impedance was measured using a frequency generator/analyzer (Solartron, FRA 1260) controlled by a personal computer. Impedance spectra were obtained at frequencies between 10 kHz and 0.1 Hz with ten steps per decade.

3. Results and discussion

3.1. Steady-state operation of a PEM fuel cell

3.1.1. Effects of operation temperature on fuel cell performance

Fig. 1 illustrates the polarization curves of a fuel cell at several operating temperatures between 65 and 85 °C with anode and cathode stoichiometric ratio of 2. These curves indicate that fuel cell performance was improved with increasing temperatures from 65 to 75 °C, unchanged between 75 and 80 °C, and begins to decrease at 85 °C. The increase in fuel cell performance between 65 and 75 °C can be explained by the

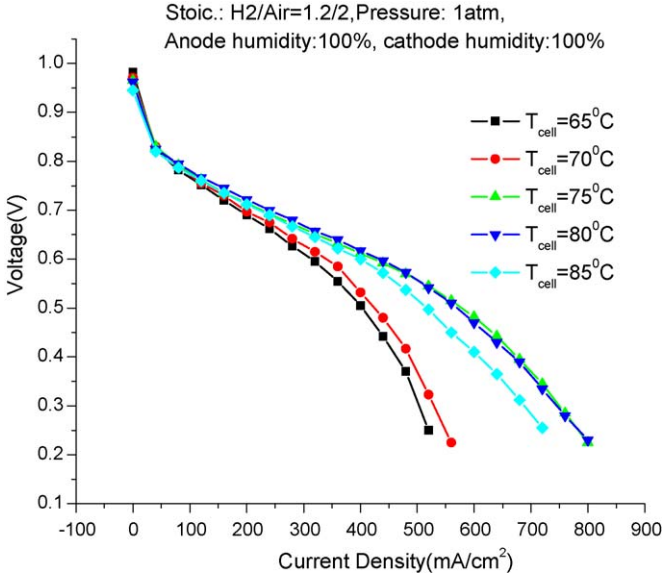

Fig. 1. Influence of the fuel cell temperature on the performance of fuel cell (25 cm^2 fuel cell with triple-serpentine flow pattern, hydrogen stoichiometry = 1.2, air stoichiometry = 2).

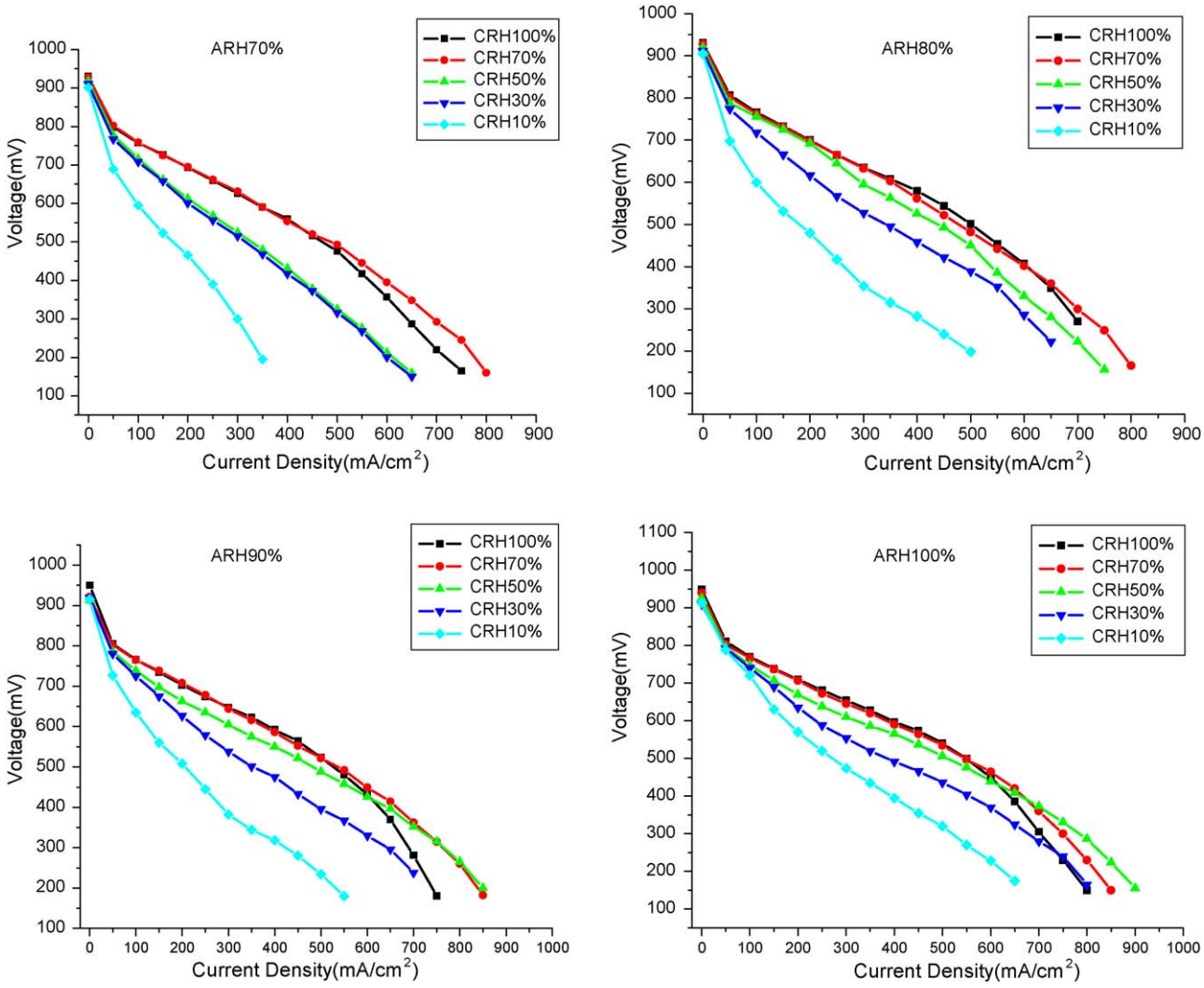

Fig. 2. Polarization curves as function of feed gas humidity fuel cell (25 cm^2 fuel cell with triple-serpentine flow pattern, hydrogen stoichiometry = 1.2, air stoichiometry = 2).

increase in the gas diffusivity and membrane conductivity at higher temperatures. Water is easily condensed at lower temperatures; water flooding may deteriorate gas diffusivity in the catalyst layer and gas diffusion layer (GDL). The gas diffusivity of the fuel cell is improved with increased fuel cell temperature; therefore, fuel cell performance is improved at higher temperatures. However, membrane conductivity decreases at high temperatures because of the reduction in the relative humidity of reactant gases and water content in the membrane. Therefore, the fuel cell performance was worse when the temperature was increased to 85 °C. As the temperature increases, there will be a greater rate of water evaporation. When the temperature reaches a critical temperature where the amount of evaporated water exceeds the amount of produced water, the membrane will start to dry out. The resistance will increase as the membranes dried out and thereby, decreases both the current and the water production. The reduced water production will cause the membrane to dry out even faster.

3.1.2. *Effect of humidity on fuel cell performance*

The polarization curves for different operating levels of air and hydrogen relative humidity are shown in Fig. 2. As seen in Fig. 2, the best case performance for low air humidity levels occurred when the hydrogen was at its highest humidity level. This observation is consistent with the results of Nguyen and White [19] who found that at high current density the transport from the anode by electro-osmotic drag exceeds transport to the anode by back diffusion from the cathode; thus, leading to membrane dehydration and performance degradation. Low humidity air can exacerbate this effect by reducing the rate of back diffusion from the cathode. Humidification of the anode gases helps to counteract this effect leading to higher performance at high levels of anode humidification. Fig. 2 also shows the polarization curves for the fuel cell at different operating levels of hydrogen humidity. The trend toward improved fuel cell performance with higher humidity levels of hydrogen was not observed. Similarly, for high relative humidity levels of air, the performance was only marginally improved with increased hydrogen humidifica-

tion. These results suggest that with the medium and high levels of air humidification, there is sufficient back diffusion to keep the membrane hydrated and that further humidification of the anode did not significantly improve the performance. Overall, the best performance occurred at low air relative humidity and high hydrogen relative humidity.

The membrane resistance was acquired by measuring the ac impedance of the fuel cell while operating at various feed gas humidity levels. For each humidity level, the membrane resistance was measured at current densities from 100 to 500 mA cm^{-2}. The contact resistance of the tested fuel cell was considered negligible since the membrane resistance is significantly larger. The resistance measurements were performed at a fuel cell temperature of 80 °C while the humidity of the air was varied from 30% to 100% and the humidity of the hydrogen was varied from 80% to 100%. Fig. 3 shows the results of the fuel cell internal resistance as a function of feed gas humidity. The graph in Fig. 3 shows that an increasing membrane resistance is a function of a decreasing feed gas relative humidity (RH). The fuel cell internal resistance increased when the air inlet RH was decreased in steps from 100% to 30% while the hydrogen inlet relative humidity was maintained at 100%. The resistance values when the fuel cell was operated at a 400 mA cm^{-2} current density included: 0.189 Ω cm^2 at 100% RH, 0.191 Ω cm^2 at 70% RH, 0.264 Ω cm^2 at 50% RH, and 0.376 Ω cm^2 at 30% RH. Membrane ionic resistance increased slightly when the hydrogen inlet RH was reduced from 100% to 80% while the air inlet RH was maintained at 100% and 70%. However, when the hydrogen inlet RH was set at 80% and the air inlet RH was reduced to 50% and 30%, the ionic resistance increased significantly from 0.263 and 0.376 to 0.383 and 0.517 Ω cm^2 at 400 mA cm^{-2}.

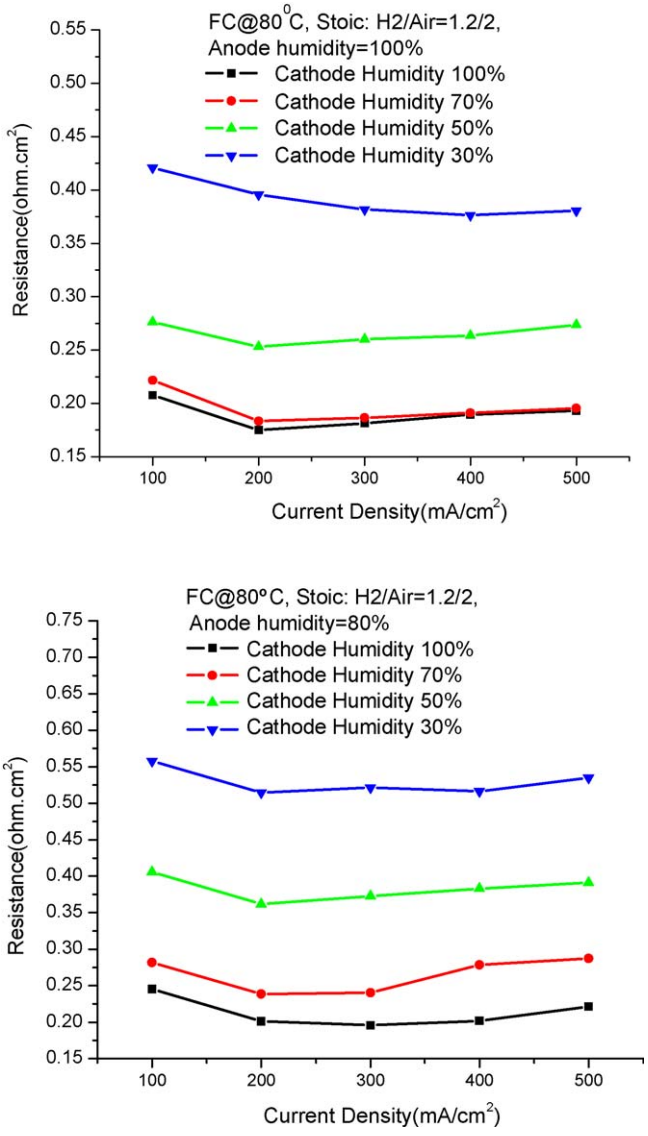

Fig. 3. Fuel cell internal resistances at different feed gas humidity: (a) anode hydrogen RH = 100%, (b) anode hydrogen RH = 80% (25 cm^2 fuel cell with triple-serpentine flow pattern, hydrogen stoichiometry = 1.2, air stoichiometry = 2).

3.1.3. Effects of feed gas stoichiometry

It is evident from Fig. 4 that as the cathode air stoichiometry increased, the fuel cell performance was improved gradually. This observation suggests that there could be an optimum cathode stoichiometry. The air stoichiometric flow rate influences both the availability of oxygen as well as the humidity of the membrane. A low air flow rate limits the availability of oxygen because the air is depleted of oxygen when it reaches the end of the air flow channels. Low air flow rate can also cause a reduction in the water removal rate (liquid and vapor) which further limits the amount of oxygen that reaches the membrane. Both of these conditions combine to reduce the performance of the fuel cell at low air flow. However, a low air flow rate increases the humidity of the membrane, which decreases the electrical resistance and improves the performance of the fuel cell. A high air flow rate increases the rate of water removal that causes drying of the membrane which increases the electrical resistance. However, the high air flow rate increases the availability of oxygen at the cathode membrane which improves the performance of the fuel cell. The increased gas flow rate is beneficial to fuel cell operation if the positive effects of increased availability of oxygen offset the negative effects of membrane dehydration.

These conditions cause the fuel cell to have an optimal air flow rate that depends on current. An air flow rate higher than the optimal air flow rate is shown to have very little influence at low currents. The electrical resistance is only a small part of the membrane losses at low currents and even though high air flow will dry out the membrane and thereby increase the electrical resistance, the voltage will only be marginally reduced. The air flow rate will have a stronger influence at higher currents when the electrical resistance is of a greater magnitude. At high currents, the performance of the fuel cell will increase quickly with increasing air flow rate if the air flow rate is below the optimal air flow rate and decrease slowly if the air flow rate increases beyond the optimal value.

3.1.4. Effect of pressure on fuel cell performance

Pressure is another operating parameter that has significant effects on fuel cell performance. Fuel cell parameters, such as inlet gas compositions and the diffusivities of the GDL, may change with the reactant gas pressures. In this study,

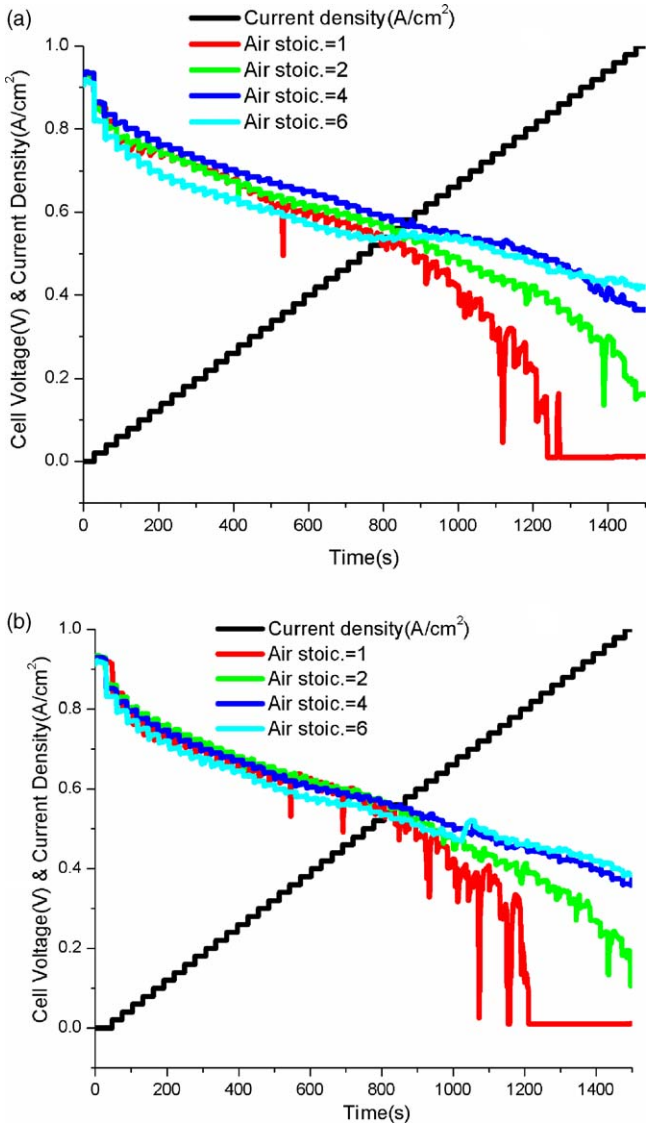

Fig. 4. The effect of air stoichiometry on fuel cell performance (25 cm^2 fuel cell with triple-serpentine flow pattern, fuel cell temperature = 80 °C, hydrogen stoichiometry = 1.2, anode hydrogen RH = 100%, cathode air RH = 80% (a), air RH = 60% (b), fuel cell system at atmosphere pressure).

the fuel cell operating temperature was kept at 80 °C, while the pressure was varied from 1 to 4 atm. Since the saturation pressure does not vary for constant operating temperature, the mole fraction of water vapor decreases with increasing total pressure. However, the mole fraction of oxygen increases with increasing operating pressure. The polarization curves of different fuel cell operating pressures are shown in Fig. 5. As the operating pressure was increased from 1 to 4 atm, the fuel cell performance also improved.

3.2. Fuel cell transient response to current steps under various operation conditions

3.2.1. Fuel cell transient behavior under different air humidity

Fuel cell performance was significantly influenced by the membrane humidity. It is difficult to measure the humidity of

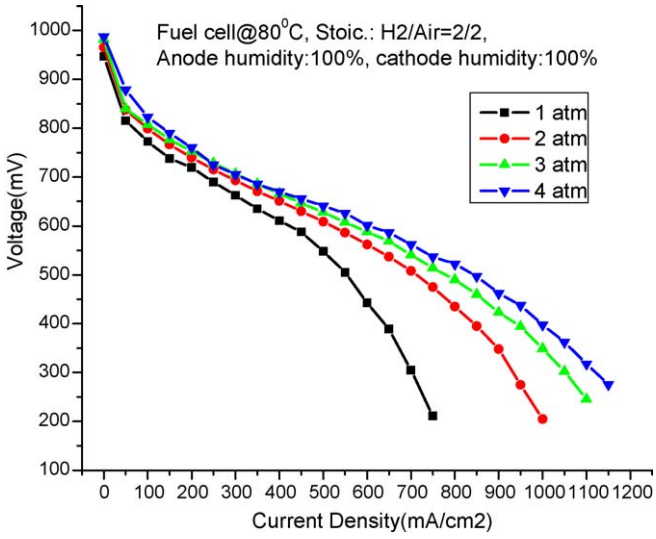

Fig. 5. The effects of air pressure on fuel cell performance (25 cm^2 fuel cell with triple-serpentine flow pattern, hydrogen stoichiometry = 1.2, air stoichiometry = 2).

gas inside the fuel cell flow channels. However, the hydrogen and air humidity can be controlled before entering the flow channels and significantly affects the fuel cell performance [46]. The experiments with different levels of air humidity have been done to determine the effect on the fuel cell dynamic performance. The air humidity was controlled from 0% (dry gas) to approximately 100% RH at 80 °C. Fig. 6 shows the dynamic response of fuel cell voltage to a current step increase under various operating conditions. It can be seen that the voltage response is nearly instantaneous under the fully humidified condition, while it takes several seconds for low-humidity fuel cells to attain the new steady-state voltage. In addition, the dynamic behavior of dry and other low-humidity cases exhibit high voltage undershoot when performing a current step of 100 mA cm^{-2}. The magni-

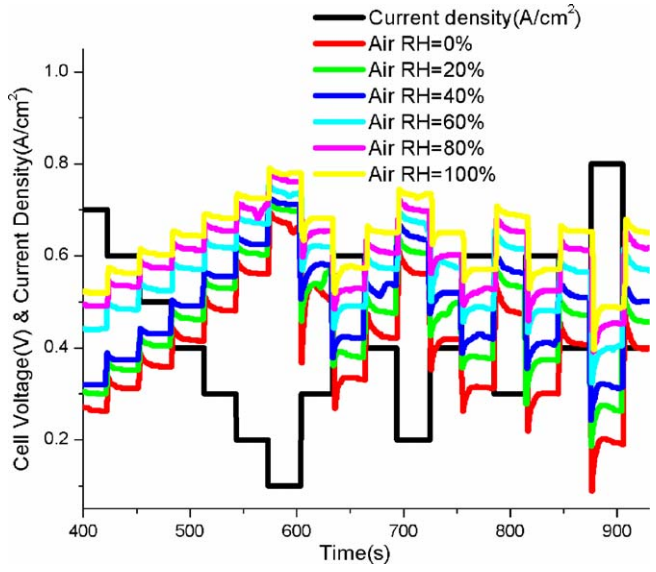

Fig. 6. Dynamic responses of the fuel cell voltage operating with different air humidity to the step changes of current density (25 cm^2 fuel cell with triple-serpentine flow pattern, hydrogen stoichiometry = 1.2, air stoichiometry = 2).

tude of undershoots increase with the current step size. When the current density changed from 0.4 to 0.8 A cm^{-2}, the fuel cell voltage undershoot dropped more than 0.15 V. With a larger current increase (i.e. >0.4 A cm^{-2}), the PEMFC voltage will reverse polarity which may lead to fuel cell degradation. This can be explained by the water electro-osmotic drag, which increases directly proportional to the current density jump.

3.2.2. Fuel cell transient behavior under different fuel cell temperatures

The polarization curves of the fuel cell at different operating temperatures are illustrated in Fig. 1. The dynamic performance of a 5 cm^2 fuel cell operating at 70 and 80 °C was compared in Fig. 7. Fig. 7 shows the transient voltage caused by current steps when the fuel cell was operating with an anode hydrogen stoichiometric ratio of 2 and air stoichiometric flow rate of 2, 3, 5 and 10. The feed gas humidity was 100% and 20% for hydrogen and air, respectively. At an operating temperature of 70 °C and air stoichiometry of 2, the fuel cell showed unstable and slower dynamic response. When the current was stepped at low current densities, the voltage undershoot of the fuel cell was 0.1–0.2 V. The fuel cell voltage reduced to zero and took more than 20 s to obtain the new steady-state voltage, and the fuel cell voltage could not recover in 30 s from its voltage reduction after current steps from the current density of 0.6–0.7 A cm^{-2}. The fuel cell dynamic response improved when the air stoichiometry was 3–5. The transient response improved at an air stoichiometric value of 10, but the absolute voltage values decrease. At the temperature of 80 °C, the fuel cell also showed unstable and slower dynamic response when the air stoichiometry is 2. The fuel cell dynamic response got better at the air stoichiometry of 3–5. At the air stoichiometry of 10, the transient response of the fuel cell required more than 20 s to achieve its new steady voltage. The fuel cell could not recover from the voltage undershoot in 30 s when performing current steps from the current density of 0.5–0.6 A cm^{-2}.

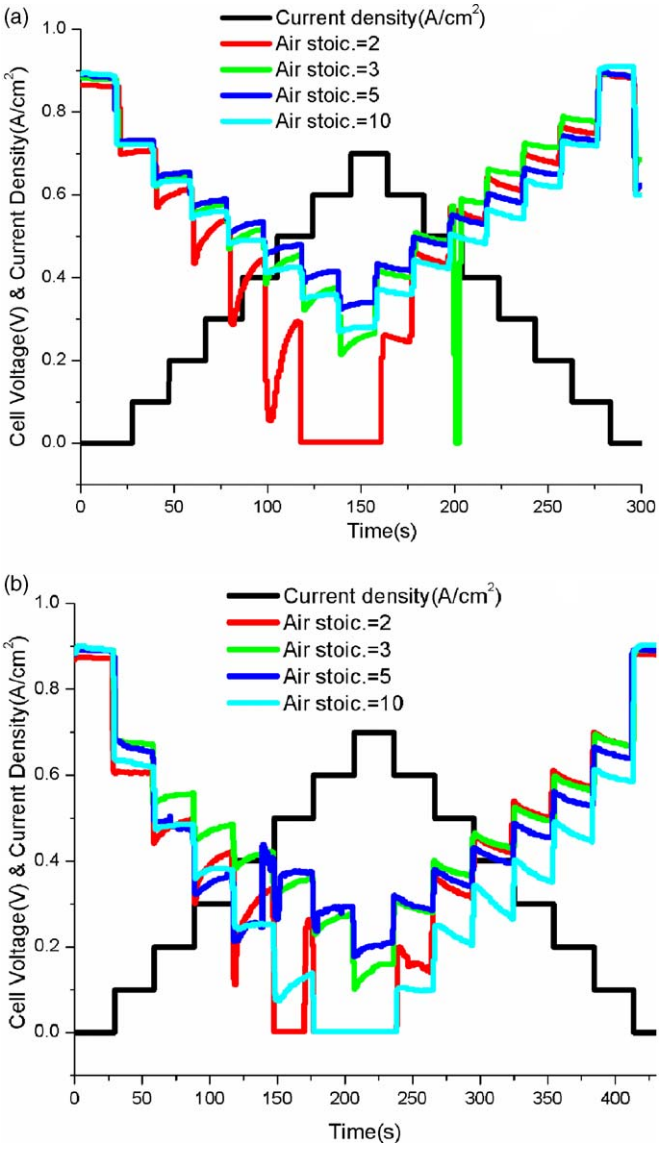

Fig. 7. The fuel cell voltage response to a current step response of 100 mA cm^{-2} under: (a) 70 °C and (b) 80 °C (5 cm^2 fuel cell with triple-serpentine flow pattern, hydrogen stoichiometry = 1.2, air stoichiometry = 2).

The fuel cell showed unstable and slower dynamic performance at lower air stoichiometry for both 70 and 80 °C. This can be explained by poor air management in the cathode side of the fuel cell. When the air stoichiometry increases to 3 and 5, the fuel cell exhibited fast and stable dynamic behavior for both temperatures. The fuel cell showed worse dynamic response at the air stoichiometry of 10 at 80 °C. This observation can be explained by the decrease of membrane conductivity at the higher temperature. Water is more easily evaporated at 80 than 70 °C; membrane dehydration may deteriorate the membrane. Membrane conductivity of the fuel cell is decreased with increasing fuel cell temperature; therefore, fuel cell dynamic performance is decreased under the conditions of higher temperature and higher air stoic. As a conclusion, operating temperature was found to have a significant effect on the steady state and dynamic performance of PEM fuel cells by its effect on membrane conductivity and water transport in GDL.

3.2.3. Fuel cell transient behavior under different air stoichiometry

Fig. 8 shows the fuel cell voltage response when the current density is changed rapidly under different air stoichiometry. Fuel cell voltage overshoot/undershoot behavior was observed after performing current steps. The air stoichiometry affects the fuel cell response as can be seen from typical fuel cell polarization curves in Fig. 4. Fig. 8 shows the effect of air stoichiometry on the fuel cell transient response under different air stoichiometry. At the air stoichiometry of 1, the fuel cell showed poor dynamic response. At low current density when the current steps up, the undershoot of fuel cell voltage reached 0.1–0.2 V even though the fuel cell showed better steady-state performance at low current density. The fuel cell exhibited poor dynamic behavior when performing current steps under high current density (0.6–1.0 A cm^{-2}), the fuel cell voltage reduces to zero and took more than 20 s to achieve its new steady voltage. The fuel cell did not recover from the voltage reduction in 30 s after current steps higher than 0.8 A cm^{-2}. The fuel cell dynamic response

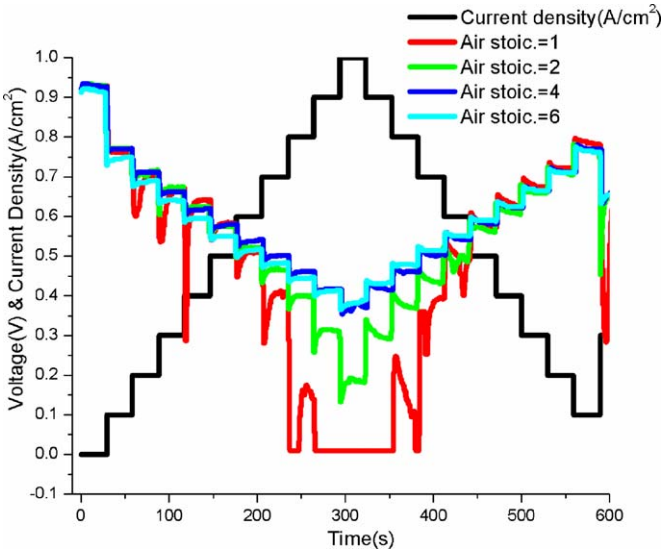

Fig. 8. The effect of air stoichiometry on fuel cell voltage (25 cm^2 fuel cell with triple-serpentine flow pattern, hydrogen stoichiometry = 1.2, fuel cell temperature = 80 °C, anode hydrogen RH = 100%, cathode air RH = 80%).

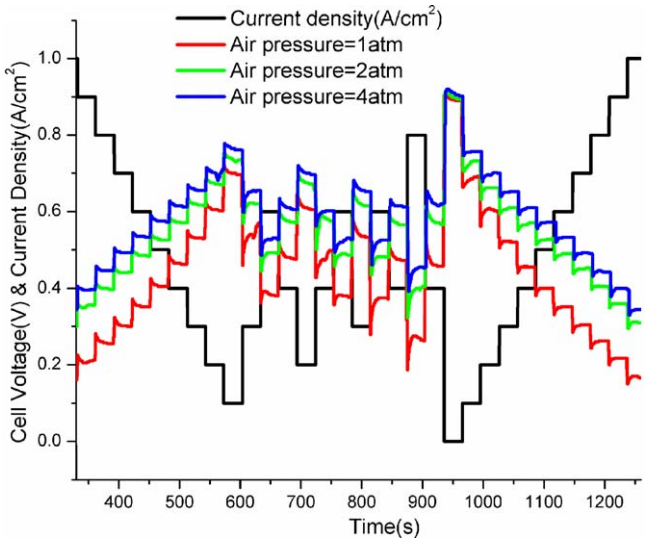

Fig. 9. The effect of cathode side pressure on fuel cell voltage response to current step conditions (25 cm^2 fuel cell with triple-serpentine flow pattern, 80 °C fuel cell temperature, air feed system at cathode pressure in bars shown in chart, anode hydrogen RH = 100%, cathode air RH = 80%).

improved at the air stoic of 2. The highest undershoot/overshoot voltage was around 0.05 V and recovery time was less than 10 s. Undershoot behaviors were observed at lower air stoichiometry. The undershoot behavior is explained by poor air management in the cathode side of the fuel cell. When the air stoichiometry increases to 4 and 6, there were no observations of overshoot or undershoot behaviors. The fuel cell responded in a fast, stable dynamic behavior. The higher air stoichiometry provided a rapid and stable response under dynamic loaded operation and the lower air stoichiometry had poor performance and slow transient response. This is in agreement with the steady-state performance data (Fig. 4). The lower air stoichiometry results in an electrically unstable response from the fuel cell. This response may be attributed to the oxygen mass transfer problem in the GDL and catalyst layer in the cathode side of the fuel cell, such as oxygen starvation or water flooding. The fast achievement of steady-state conditions at the higher air stoichiometries can be attributed to the enhanced water removal and faster oxygen transports in the fuel cell cathode side. The higher air stoichiometries vaporize more water.

It can be concluded that the flow rate does not significantly affect the fuel cell dynamic response in the case of low to middle current densities and when current changes are gradual. On the contrary, when the fuel cell is operated at high current densities and when sudden higher current step changes in the fuel cell loading condition take place, the fuel cell response time is significantly affected by the air stoichiometric flow rate.

3.2.4. Fuel cell transient behavior under different air pressure

The effects of air pressure on the fuel cell performance while operating at steady state can be seen from the fuel cell polarization curves in Fig. 5. Fig. 9 illustrates the dynamic response of the fuel cell voltage at different cathode pressures. For each cathode pressure, the fuel cell was dynamically loaded by stepping the fuel cell operating current. The best response to the dynamic load was observed at the largest cathode air pressure. The effect of cathode pressure on the fuel cell response is small when compared to that of air stoichiometry and air humidity for low to medium current densities (0–600 A cm^{-2}). The effect of cathode pressure on fuel cell transient response was not significant for small current steps. A small current step of 0.1A cm^{-2} enabled the fuel cell to rapidly obtain a steady-state voltage with minimal undershoot/overshoot. The voltages undershoot/overshoot gradually increased when the magnitude of the current steps increased in increments from 0.1 to 0.4 A cm^{-2}.

Fig. 9 also illustrates the effect of cathode air pressure on the dynamic response of the fuel cell operating at large current densities and responding to large current steps. The dynamic response of the fuel cell in relation to cathode pressure is noticeably different at the higher current densities than at the lower current densities. At the air pressure of 1 atm, the transient response is slower and the fuel cell voltage overshoot/undershoot is higher than that of the larger cathode pressures. It takes approximately 15–20 s for the fuel cell to reach its new steady-state performance after the current steps. When the fuel cell is operating at the large cathode pressures, it shows a faster and more stable response to large current steps. As seen in Fig. 9, with the load cycle used in this experiment, there is approximately a 120 mV reduction in voltage when comparing the operation of the fuel cell at the lowest and highest air pressures.

According to the results in Figs. 5 and 9, the steady state and dynamic response of the fuel cell are both improved by operating the cathode at high pressures. A contributing factor to this behavior is the effect of higher cathode pressure reducing the mass transfer over potential at the cathode. Dynamic performance operating at different air pressures is in accordance with the steady-state performance data shown in Fig. 5. The difference in voltage over the range of air pressure increases as the magnitude of the current load increases. The major difference

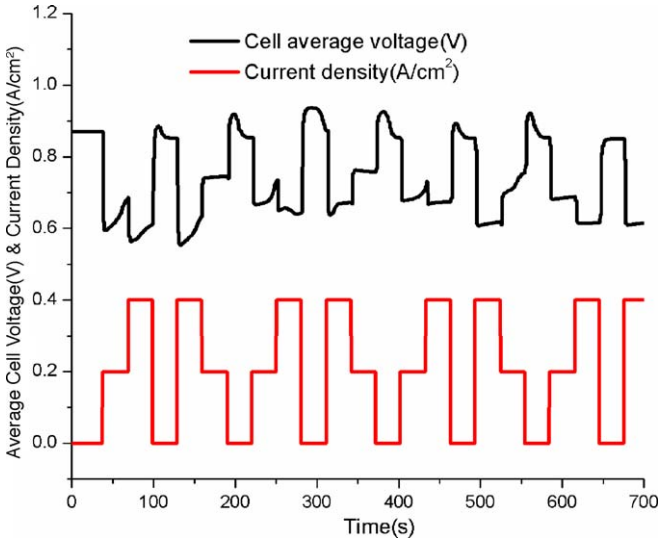

Fig. 10. The transient response of a eight-cell stack to output current steps (50 cm^2 triple-serpentine single fuel cell, stack operating at room temperature, feed gases without humidified, feed gases at atmospheric pressure, hydrogen stoichiometry = 1.2, air stoichiometry = 2).

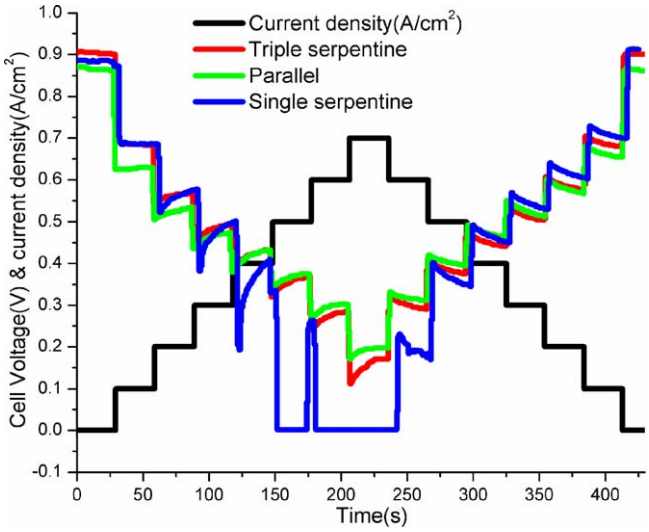

Fig. 11. The transient behavior of the fuel cells with different types of flow-field design (5 cm^2 fuel cells with single serpentine, triple-serpentine and parallel flow patterns, fuel cell working temperature at 80 °C, anode hydrogen RH = 100%, cathode air RH = 80%, feed gases at atmospheric pressure, hydrogen stoichiometry = 1.2, air stoichiometry = 2).

between the responses shown in Fig. 9 is the time required for the fuel cell to reach a new steady-state voltage while operating at the lowest air pressure.

3.2.5. Dynamic response of a eight membrane fuel cell stack to output current steps

The transient response of the stack to output current steps has been measured, and this response is illustrated in Fig. 10. This paper reports the effect of varying loads on an eight membrane PEM fuel cell stack. Each membrane used to construct the stack had an active area of 50 cm^2. The stack transient voltage response to a load variation is similar to the single fuel cell behavior; however, the transient magnitude is proportional to the size of the load current steps. This relationship between transient magnitude and load current step was not observed in the single fuel cell tests. The transient responses of the average fuel cell voltage have been investigated to obtain information on the dynamic characteristics of the stack.

3.2.6. Gas channel pattern

The types of flow field pattern design affect the steady state and dynamic response of the fuel cell. The process of selecting the fuel cell flow design must consider the operating environment of the fuel cell. If the fuel cell is used for stationary applications, the steady-state response is more important than the transient response. However, if the fuel cell is used for automobile applications, the transient and steady state responses are important to the selection of the flow channel design. The transient behavior of the different flow-field designs were investigated in this report (Fig. 11). Several flow-field designs, including the (1) single serpentine, (2) parallel, and (3) triple-serpentine, were evaluated during steady state and transient load conditions. The transient responses of three 5 cm^2 single membrane fuel cells were studied by changing the current density from 0 to 0.70 A cm^{-2} with a current step of 0.1 A cm^{-2}. The fuel cell voltage response was recorded during each current step. Initially when the load level was increased, the voltage suddenly dropped and then increased to a value slightly higher than the dropped value. It was observed that the parallel flow design gave the best transient performance, especially at higher current density, while the transient performance was poor for the single serpentine design. As discussed above, the single serpentine type of design gave the best steady-state performance at low current density; however, it also gave the worse transient performance especially at higher current densities. The parallel flow field design gave the lowest steady-state performance, but it also had the best transient performance. The triple serpentine type of flow-field design performed well for both the steady state and transient performance. These experimental results prove that the overall performance of the fuel cell depends on the flow channel design.

4. Conclusions

The steady-state performance and transient response of single membrane H_2/air PEM fuel cells and a stack were investigated under a variety of loading cycles and operating conditions. Different feed gas humidity, operation temperature, feed gas stoichiometry, air pressure, fuel cell size and gas flow patterns were found to affect both the steady state and dynamic response of the PEM fuel cells. It was found that the humidity in both the anode and cathode inlet gases had a significant effect on fuel cell performance. The experimental results have shown that a decrease in the cathode humidity has a detrimental effect on the fuel cell steady state and dynamic performance. Temperature was found to have a significant effect on the PEM fuel cell performance by its effect on membrane humidity and water transport in the GDL and catalyst layer. The polarization curves of the fuel cell at different operating temperatures showed that fuel cell performance was improved with increasing temperature

from 65 to 75 °C. The air stoichiometric flow rate also influenced the performance of the fuel cell directly by supplying oxygen and indirectly by influencing the humidity of the membrane and water flooding in cathode side. Experiments showed that an optimum air stoichiometry exists that is much larger than the stoichiometric value required for oxidation of the fuel. The fuel cell steady state and dynamic performance also improved as the operating pressure was increased from 1 to 4 atm. The types of flow field pattern design were found to affect both the steady state and dynamic response of the fuel cell. Based on the experimental results, both the steady state and dynamic response of the fuel cells were analyzed. This experimental data will provide a baseline for validation of fuel cell models.

Acknowledgment

This project is generously supported by the Center for Advanced Vehicular Systems (CAVS) at Mississippi State University.

References

[1] D. Oliver, J. Murphy, G. Duncan Hitchens, D.J. Manko, J. Power Sources 47 (1994) 353–368.
[2] S.J.C. Cleghorn, X. Ren, T.E. Springer, M.S. Wilson, C. Zawodzinski, T.A. Zawodzinski, S. Gottesfeld, Int. J. Hydrogen Energy 22 (1997) 1137–1144.
[3] Prater FK.B., J. Power Sources 61 (1996) 105–109.
[4] Z.-G. Zhang, G. Xu, X. Chen, K. Honda, T. Yoshida, Process development of hydrogenous gas production for PEFC from biogas, Fuel Process. Technol. 85 (2004) 1213–1229.
[5] B.C.H. Steele, Material science and engineering: the enabling technology for the commercialisation of fuel cell systems, J. Mater. Sci. 36 (2001) 1053–1068.
[6] J. Xie, D.L. Wood III, D.M. Wayne, T.A. Zawodzinski, P. Atanassov, R.L. Borup, Durability of PEFCs at high humidity conditions, J. Electrochem. Soc. 152 (2005) A104–A113.
[7] J.T. Pukrushpan, A.G. Stefanopoulou, H. Peng, Control of Fuel Cell Power Systems: Principles, Modeling Analysis and Feedback Design, Springer, 2004, ISBN 1-85233-816-4 (XVII).
[8] M. Grujicic, K.M. Chittajallu, Appl. Surf. Sci. 227 (2004) 56–72.
[9] J. Hamelin, K. Agbossou, A. Laperriere, F. Laurenfuel celle, T.K. Bose, Dynamic behavior of a PEM fuel cell stack for stationary applications, Int. J. Hydrogen Energy 26 (6) (2001) 625–629.
[10] S.O. Morner, S.A. Klein, Experimental evaluation of the dynamic behavior of an air-breathing fuel cell stack, J. Solar Energy Eng. 123 (3) (2001) 225–231.
[11] S. Kim, S. Shimpalee, J.W. Van Zee, The effect of stoichiometry on dynamic behavior of a proton exchange membrane fuel cell (PEMFC) during load change, J. Power Sources 135 (1/2) (2004) 110–121.
[12] S. Kim, S. Shimpalee, J.W. Van Zee, The effect of reservoirs and fuel dilution on the dynamic behavior of a PEMFC, J. Power Sources 137 (1) (2004) 43–52.
[13] P. Argyropoulos, K. Scott, W.M. Taama, Dynamic response of the direct methanol fuel cell under variable load conditions, J. Power Sources 87 (2000) 153–161.
[14] P. Argyropoulos, K. Scott, W.M. Taama, The effect of operating conditions on the dynamic response of the direct methanol fuel cell, Electrochim. Acta 45 (2000) 1983–1998.
[15] T.E. Springer, T.A. Zawodzinski, S. Gottesfeld, Polymer electrolyte fuel cell model, J. Electrochem. Soc. 138 (8) (1991) 2334–2342.
[16] D.M. Bernardi, M.W. Verbrugge, A mathematical model of the solid-polymer-electrolyte fuel cell, J. Electrochem. Soc. 139 (9) (1992) 2477–2491.
[17] D.M. Bernardi, M.W. Verbrugge, Mathematical model of a gas-diffusion electrode bonded to a polymer electrolyte, AIChE J. 37 (1991) 1151–1163.
[18] T.F. Fuller, J. Newman, Water and thermal management in solid-polymer-electrolyte fuel cells, J. Electrochem. Soc. 140 (5) (1993) 1218–1225.
[19] T.V. Nguyen, R.E. White, A water and heat management model for proton-exchange-membrane fuel cells, J. Electrochem. Soc. 140 (8) (1993) 2178–2186.
[20] V. Gurau, H. Liu, S. Kakac, Two-dimensional model for proton exchange membrane fuel cells, AIChE J. 44 (11) (1998) 2410–2422.
[21] J.T. Wang, R.F. Savinell, Simulation studies on the fuel electrode of a hydrogen–oxygen polymer electrolyte fuel cell, Electrochim. Acta 37 (15) (1992) 2737–2745.
[22] J.S. Yi, T.V. Nguyen, An along-the-channel model for proton exchange membrane fuel cells, J. Electrochem. Soc. 145 (4) (1998) 1149–1159.
[23] W. He, J.S. Yi, T.V. Nguyen, Two-phase flow model of the cathode of PEM fuel cells using interdigitated flow fields, AIChE J. 46 (2000) 2053–2064.
[24] J.C. Amphlett, R.F. Mann, B.A. Peppley, P.R. Roberge, A. Rodrigues, J. Power Sources 61 (1/2) (1996) 183–188.
[25] J.C. Amphlett, E.H. de Oliveira, R.F. Mann, P.R. Roberge, A. Rodrigues, J.P. Salvador, Dynamic interaction of a proton exchange membrane fuel cell and a lead-acid battery, J. Power Sources 65 (1/2) (1997) 173–178.
[26] S. Um, C.-Y. Wang, K.S. Chen, Computational fluid dynamics modeling of proton exchange membrane fuel cells, J. Electrochem. Soc. 147 (12) (2000) 4485–4493.
[27] M. Ceraolo, C. Miulli, A. Pozio, Modelling static and dynamic behavior of proton exchange membrane fuel cells on the basis of electro-chemical description, J. Power Sources 113 (1) (2003) 131–144.
[28] K. Sundmacher, T. Schultz, S. Zhou, K. Scott, M. Ginkel, E.D. Gilles, Dynamics of the direct methanol fuel cell (DMFC): experiments and model-based analysis, Chem. Eng. Sci. 56 (2001) 333–341.
[29] A.A. Kulikovsky, Gas dynamics in channels of a gas-feed direct methanol fuel cell: exact solutions, Electrochem. Commun. 3 (2001) 572–579.
[30] C. Xu, P.M. Follmann, L.T. Biegler, M.S. Jhon, Numerical simulation and optimization of a direct methanol fuel cell, Comput. Chem. Eng. 29 (2005) 1849–1860.
[31] T. Berning, N. Djilali, A 3D, multiphase, multicomponent model of the cathode and anode of a PEM fuel cell, J. Electrochem. Soc. 150 (12) (2003) A1589–A1598.
[32] X. Xue, J. Tang, A. Smirnova, R. England, N. Sammes, System level lumped-parameter dynamic modeling of PEM fuel cell, J. Power Sources 133 (2) (2004) 188–204.
[33] S. Shimpalee, W.-K. Lee, J.W. Van Zee, H. Naseri-Neshat, Predicting the transient response of a serpentine flow-field PEMFC. I. Excess to normal fuel and air, J. Power Sources 156 (2006) 355–368.
[34] S. Shimpalee, W.-K. Lee, J.W. Van Zee, H. Naseri-Neshat, Predicting the transient response of a serpentine flow-field PEMFC. II. Normal to minimal fuel and air, J. Power Sources 156 (2006) 369–374.
[35] X. Yu, B. Zhou, A. Sobiesiak, Water and thermal management for Ballard PEM fuel cell stack, J. Power Sources 147 (1/2) (2005) 184–195.
[36] Y. Wang, C.-Y. Wang, Transient analysis of polymer electrolyte fuel cells, Electrochim. Acta 50 (6) (2005) 1307–1315.
[37] Y. Wang, C.-Y. Wang, Dynamics of polymer electrolyte fuel cells undergoing load changes, Electrochim. Acta, in press.
[38] S. Enback, G. Lindbergh, Experimentally validated model for CO oxidation on PtRu/C in a porous PEFC electrode, J. Electrochem. Soc. 152 (1) (2005) A23–A31.
[39] H. Ju, C.-Y. Wang, Experimental validation of a PEM fuel cell model by current distribution data, J. Electrochem. Soc. 151 (11) (2004) A1954–A1960.
[40] J.J. Baschuk, X. Li, Modelling CO poisoning and O_2 bleeding in a PEM fuel cell anode, Int. J. Energy Res. 27 (2003) 1095–1116.
[41] P. Costamagna, E. Arato, E. Achenbach, U. Reus, Fluid dynamic study of fuel cell devices: simulation and experimental validation, J. Power Sources 52 (2) (1994) 251–260.

[42] M. Noponen, E. Birgersson, J. Ihonen, M. Vynnycky, A. Lundblad, G. Lindbergh, A two-phase non-isothermal PEFC model: theory and validation, Fuel Cells (Weinheim, Germany) 4 (4) (2004) 365–377.
[43] N.P. Siegel, M.W. Ellis, D.J. Nelson, M.R. von Spakovsky, A two-dimensional computational model of a PEMFC with liquid water transport, J. Power Sources 128 (2) (2004) 173–184.
[44] M.M. Mench, C.Y. Wang, M. Ishikawa, In situ current distribution measurements in polymer electrolyte fuel cells, J. Electrochem. Soc. 150 (8) (2003) A1052–A1059.
[45] J. St.-Pierre, J. Roberts, K. Colbow, S. Campbell, A. Nelson, J. New Mater. Electrochem. Syst. 8 (3) (2005) 163–176.
[46] Q. Yan, J. Wu, Q. Liu, Experiments toward fundamental validation of PEM fuel cell models, in: Proceeding of the Third International Conference on Fuel Cell Science, Engineering and Technology, Ypsilanti, MI, May 23–25, 2005, pp. 183–190.